



HAL
open science

Internal Rotation of OH Group in 4-Hydroxy-2-butyne nitrile Studied by Millimeter-Wave Spectroscopy

Roman A Motiyenko, Laurent Margulès, Maria L Senent, Jean-Claude
Guillemin

► **To cite this version:**

Roman A Motiyenko, Laurent Margulès, Maria L Senent, Jean-Claude Guillemin. Internal Rotation of OH Group in 4-Hydroxy-2-butyne nitrile Studied by Millimeter-Wave Spectroscopy. *Journal of Physical Chemistry A*, 2018, 122 (12), pp.3163-3169. 10.1021/acs.jpca.7b12051 . hal-01771512

HAL Id: hal-01771512

<https://univ-rennes.hal.science/hal-01771512>

Submitted on 3 May 2018

HAL is a multi-disciplinary open access archive for the deposit and dissemination of scientific research documents, whether they are published or not. The documents may come from teaching and research institutions in France or abroad, or from public or private research centers.

L'archive ouverte pluridisciplinaire **HAL**, est destinée au dépôt et à la diffusion de documents scientifiques de niveau recherche, publiés ou non, émanant des établissements d'enseignement et de recherche français ou étrangers, des laboratoires publics ou privés.

1
2
3
4
5
6
7
8
9
10
11
12
13
14
15
16
17
18
19
20
21
22
23

Internal rotation of OH group in 4-hydroxy-2-butyne nitrile studied by millimeter-wave spectroscopy

Roman A. Motiyenko,^{*,†} Laurent Margulès,[†] Maria L. Senent,[‡] and Jean-Claude
Guillemin^{*,¶}

[†]*Laboratoire de Physique des Lasers, Atomes et Molécules, UMR 8523, CNRS - Université
de Lille, F-59655 Villeneuve d'Ascq Cedex, France*

[‡]*Departamento de Química y Física Teóricas, Instituto de Estructura de la Materia,
IEM-C.S.I.C., Serrano 121, Madrid 28006, Spain*

[¶]*Univ Rennes, École Nationale Supérieure de Chimie de Rennes, CNRS, ISCR -
UMR6226, F-35000 Rennes, France*

E-mail: roman.motienko@univ-lille1.fr; jean-claude.guillemin@ensc-rennes.fr

Phone: +33(0)320434490. Fax: +33(0)320337020

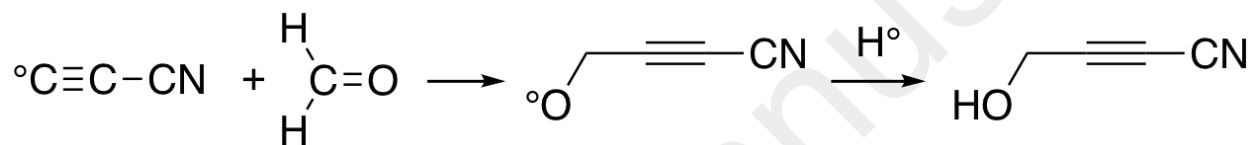
Abstract

Cyanoacetylene, HCC–CN is a ubiquitous molecule in the Universe. **However, its interstellar chemistry is not well understood and its understanding requires laboratory data including rotational spectroscopy of possible products coming from a reaction with another compounds.** In this study we present the first spectroscopic characterization of *gauche* conformation of 4-hydroxy-2-butyne nitrile (HOCH₂CCCN), **a formal adduct of cyanoacetylene on formaldehyde**, in the frequency range up to 500 GHz. The analysis of the rotational spectrum was complicated by internal rotation of OH group that connects two equivalent *gauche* configurations. The spectral assignment was aided by high level quantum chemical calculations that were particularly useful in the interpretation of torsion-rotational part of the problem. The applied reduced-axis-system (RAS) formalism allowed fitting within experimental accuracy the lines with $K_a < 18$. We also present the method **of search for** initial global solution of torsion-rotational problem within RAS formalism. Accurate spectroscopic parameters obtained in this study provide a reliable basis for the detection of 4-hydroxy-2-butyne nitrile in the interstellar medium.

Introduction

Cyanoacetylene is a ubiquitous molecule in the Universe since it has been observed in interstellar clouds^{1–5}, Hale-Bopp comet⁶ and in the atmosphere of Titan, the largest moon of Saturn^{7,8}. Cyanoacetylene is probably the precursor of many cyanopolyynes by photolysis in the presence of acetylene or polyynes.^{9–12} **Besides** two methyl derivatives, MeC₃N and MeC₅N, which could be formed by a similar approach but with propyne or 1,3-pentadiyne^{13,14} instead of acetylene or unsubstituted polyynes, no other derivative containing the C₃N moiety has been detected in the interstellar medium (ISM). For many compounds, this could be explained by the lack of rotational spectra recorded in laboratory. However, the formal addition of ammonia, hydrogen sulfide or water which respectively gives 3-amino-2-propenenitrile,¹⁵ 3-

mercapto-2-propenenitrile¹⁶ and 3-hydroxy-2-propenenitrile (the latter rearranges in cyanoacetaldehyde)¹⁷ was studied and the rotational spectra of these adducts were recorded. At present, none of them has yet been detected to date in the ISM. Another approach of interstellar formation of C₃N derivatives involves the reaction of the C₃N radical, a species detected in the ISM,¹⁸ with another compound, and this is much more comparable to the formation of cyanopolynes than the Michael addition of nucleophiles on cyanoacetylene. In TMC-1, for example, the C₃N radical and formaldehyde have been detected.¹⁹ The addition of this radical on the carbonyl could produce 4-hydroxy-2-butyne nitrile (HOCH₂CCCN, HBN) after abstraction of one hydrogen from another compound (Scheme 1).



Scheme 1

Thus, as a first target species based on the hypothesis of interstellar compounds coming from the cyanoethynyl radical addition on an unsaturated compound, we investigated the rotational spectrum of HBN. The spectral studies were augmented by high-level quantum chemical calculations performed to aid in the interpretation of the observed spectra.

Experiment

4-Hydroxy-2-butyne nitrile has been prepared as previously reported²⁰ starting from a protected propargyl alcohol and phenyl cyanate. We recorded the rotational spectrum of HBN using fast-scan terahertz spectrometer. The details of the spectrometer except of the fast-scan feature are described by Zakharenko et al.²¹ In the present study, the spectrum was recorded in the frequency ranges 50 - 110 GHz, 150 - 195 GHz, 225 - 330 GHz and 400 - 500 GHz. As a radiation source in the spectrometer, we use commercially available frequency multiplication chains that are driven by home-made fast sweep frequency synthesizer. In the

1
2
3 frequency range 50 - 75 GHz we use active frequency multiplier x4 from Millitech. In the
4 frequency range 75 - 110 GHz the source is active multiplier x6 from VDI. At higher fre-
5 quencies, we use passive frequency multiplication of the VDI source by factors 2, 3, 5, etc.
6
7 The fast sweep system is based on the up-conversion of AD9915 direct digital synthesizer
8 (DDS) operating between 320 and 420 MHz into Ku band by mixing the signals from AD9915
9 and Agilent E8257 synthesizers with subsequent sideband filtering. The DDS provides rapid
10 frequency scan with up to 50 μ s/point frequency switching rate. Because of the HBN line
11 weakness the spectrum was scanned with slower rate of 5 ms/point or 10 ms/point depend-
12 ing on the frequency range. As an absorption cell in the spectrometer we used a stainless
13 steel tube of 10 cm in diameter, and 2 m long. Owing to good stability of the synthesized
14 sample of HBN under room temperature, the measurements were performed in a static mode
15 **with practically constant amount of the sample and consequently constant gas**
16 **pressure in the absorption cell.** Nevertheless, to minimize observations of decomposition
17 products in the spectra, the absorption cell was pumped out and refilled with new sample
18 of HBN at optimum pressure of about 20 Pa every 3-4 hours.
19
20
21
22
23
24
25
26
27
28
29
30
31
32
33
34

35 Ab initio calculations

36
37
38 Highly correlated ab initio calculations were used to determine the geometries of the two con-
39 formers, *gauche* and *trans*, and to compute low-energy torsional levels. Electronic structure
40 calculations were performed using both the MOLPRO²² and GAUSSIAN packages²³.
41
42
43

44
45 The equilibrium structures, *gauche* and *trans*, of HOCH₂CCCN, as well as the most rel-
46 evant spectroscopic parameters (equilibrium rotational constants and the one-dimensional
47 potential energy surface, 1D-PES, for the hydroxyl torsion) were computed using explic-
48 itly correlated coupled cluster theory with single and double substitutions augmented by
49 a perturbative treatment of triple excitations (CCSD(T)-F12b)^{24,25} with an aug-cc-pVTZ
50 basis set²⁶. For this purpose, we employed the MOLPRO default options. Second-order
51
52
53
54
55
56
57
58
59
60

Möller-Plesset theory (MP2) was employed to determine vibrational corrections for the potential energy surface and the α_j^r vibration-rotation constants. For the explicitly correlated calculations, the MOLPRO default options were selected.

The torsional energy levels were determined by variational calculations using the procedure previously employed for other non-rigid species²⁷. The variational procedure considers the intertransformation of the minima and the tunneling effects in the torsional barriers. If the non-rigidity is taken into account, the molecule can be classified into the Molecular Symmetry Group (MSG) G_2 . Some complementary calculations, such as the vibrational corrections, were performed using the second order perturbation theory implemented in Gaussian^{23,28}. For the latter, the two point groups C_1 and C_s were employed for the two conformers *gauche* and *trans*, respectively. The irreducible representations of G_2 can be correlated with those of C_s . Thus, the G_2 symmetric and antisymmetric representations A_1 and A_2 can be correlated with the A' and A'' representations of C_s . Previous references²⁹ describe how the internal rotation levels are correlated to the minima of the potential energy surface. For this purpose, the torsional wave functions obtained in the variational procedure were employed for computing the probability integrals. As was expected, the ground vibrational state can be confined in the absolute minima *gauche* and the A_1 component lies below the A_2 . Below the barriers where the tunneling effects are significant, once the energy increases, the relative order of subcomponents varies and the levels cannot be localized in a single minimum. Above the barriers (i.e. levels 3 and 4), tunneling effects are not present. Those levels were classified as for a semi-rigid species.

HBN displays various very low frequency vibrational modes lying in the region or below the OH torsion fundamental. They can be defined as skeletal deformations, in plane and out of plane bending modes. To estimate their band center positions, harmonic frequencies were computed using CCSD(T)-F12 the-

ory and the MOLPRO package. All these frequencies are real which assure the minimum energy character of the two conformers *gauche* and *trans*. For the *gauche* conformer, the OH harmonic torsion lies at 280 cm^{-1} , and for the *trans* conformer the band center is estimated at 194 cm^{-1} . This result is coherent with the variational calculations summarized in Figure 1. For the *gauche* form, three skeletal deformations, computed at 99 cm^{-1} , 133 cm^{-1} and 230 cm^{-1} , lie below the OH torsional fundamental. For the *trans* form, only two modes, at 100 cm^{-1} (A') and 133 cm^{-1} (A''), must be considered. A third fundamental, is computed at 237 cm^{-1} (A').

As was expected, the computation of anharmonic fundamentals using second order perturbation theory VPT2 implemented in Gaussian leads to unrealistic results for the very low energies. It has to be taken into consideration that the potential energy surface is very flat in the region of the skeletal deformations. However, it allows the estimation of possible Fermi interactions that are not expected for the OH torsion. This validates the one-dimensional model.

The ground vibrational state rotational constants of the two conformers were determined from the CCSD(T)-F12 equilibrium parameters using Equation 1

$$B_0 = B_e + \Delta B_e^{core} + \Delta B_{vib}, \quad (1)$$

This equation has been previously tested for other species using explicitly correlated methods.³⁰ Here, ΔB_e^{core} , regards the core-valence-electron correlation effect on the equilibrium parameters. It was computed at the CCSD(T) level of theory³¹ as the difference between $B_e(CV)$, (calculated correlating both core and valence electrons) and $B_e(V)$ (calculated correlating just the valence electrons). The vibrational contribution ΔB_{vib} was computed with MP2 and second order perturbation theory. The results for the two conformers are shown in Table 1.

Table 1: Calculated equilibrium and ground-state rotational constants (MHz), energies and conformational barriers (cm⁻¹), and dipole moments (Debye) for HOCH₂CCCN.

Parameter	<i>gauche</i> -HOCH ₂ CCCN	<i>trans</i> -HOCH ₂ CCCN
A_e	26032.92	27964.26
B_e	1321.39	1320.38
C_e	1270.95	1270.90
A_0	25989.27	27997.46
B_0	1325.56	1326.98
C_0	1273.50	1272.18
ΔE		447.3
$V(\textit{gauche-gauche})$		325.7
$V(\textit{gauche-trans})$		522.2
μ	4.21	6.33
μ_a	3.85	5.91
μ_b	1.13	2.26
μ_c	1.25	0.0

The low torsional energy levels were calculated using a variational solution of the Hamiltonian given in Equation 2^{32,33}:

$$\hat{H}(\alpha) = - \left(\frac{\partial}{\partial \alpha} \right) B_\alpha \left(\frac{\partial}{\partial \alpha} \right) + V^{eff}(\alpha). \quad (2)$$

Here, α is the OH torsional coordinate, B_α are the kinetic energy parameters, and $V^{eff}(\alpha)$ is the vibrationally corrected 1D-PES²⁹ shown in Figure 1.

The ground vibrational state splits into two components $E(0^-)$ and $E(0^+)$ because of tunneling in the $V(\textit{gauche-gauche})$ barrier. Ab initio calculations predict a splitting of 173280 MHz (5.78 cm⁻¹). In addition, the first excited vibrational state shows two components lying at 278.5 cm⁻¹ (1^+) and 322.6 cm⁻¹ (1^-) over the ground state. The first *trans* level lies at 439 cm⁻¹ (0), see Figure 1.

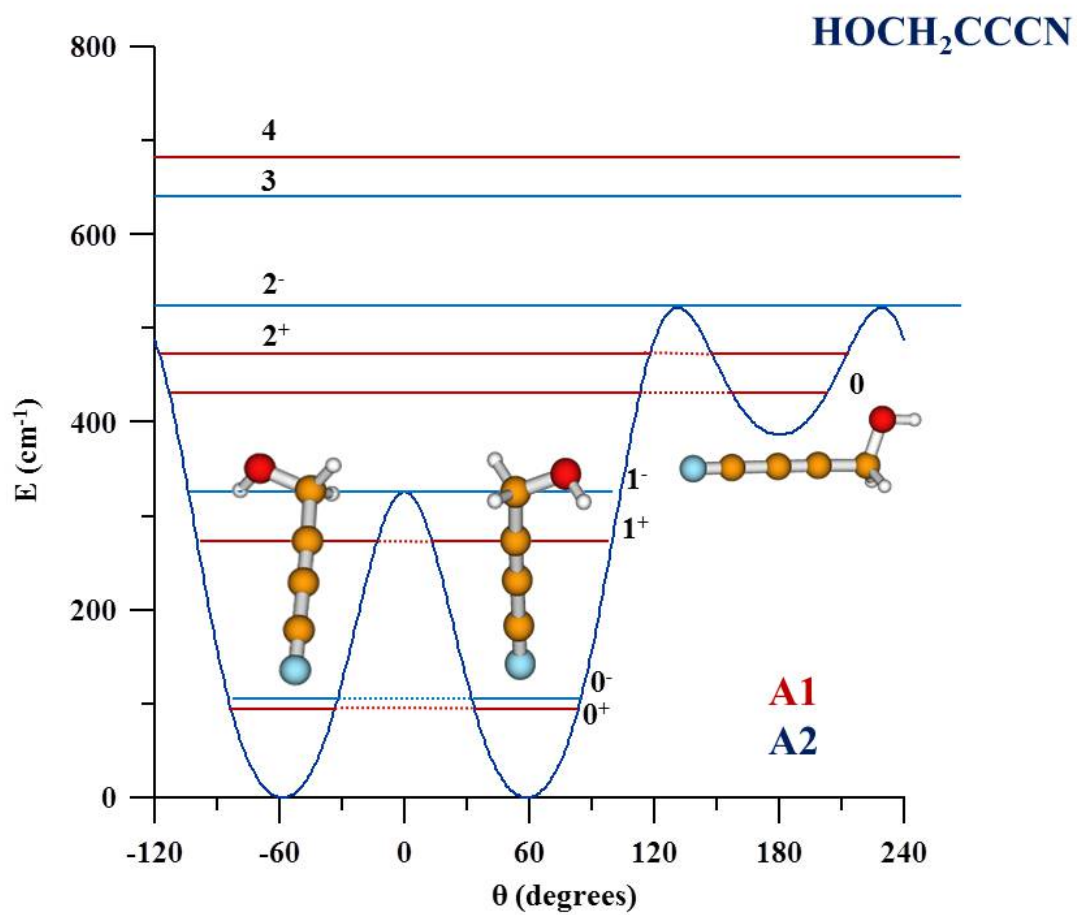


Figure 1: CCSD(T)-F12 potential energy of HBN as a function of the hydroxyl group internal rotation coordinate

Analysis and Discussion

In this study, we assigned and analyzed the rotational spectrum of the most stable *gauche* conformation, as it represents the highest interest from the point of view of subsequent interstellar searches. The initial assignment of the rotational spectrum of *gauche*-HBN was based on the results of quantum chemical calculations. The initial predictions were calculated using theoretical values of rotational and centrifugal distortion constants. The predictions allowed relatively easy assignment of the band origins of strong series of ${}^aR_{0,1}$ transitions owing to high value of μ_a dipole moment component. An example of such series is shown on Fig. 2. Comparison between theoretical and experimental band origins provided first corrections to the rotational constants B and C , as the difference between two consecutive band origins is approximately equal to $B+C$. At the next step, using the corrected frequency predictions, we assigned low K_a transitions with $K_a < 3$. As expected, such transitions exhibited doublet structure owing to tunneling through the barrier to OH internal rotation.

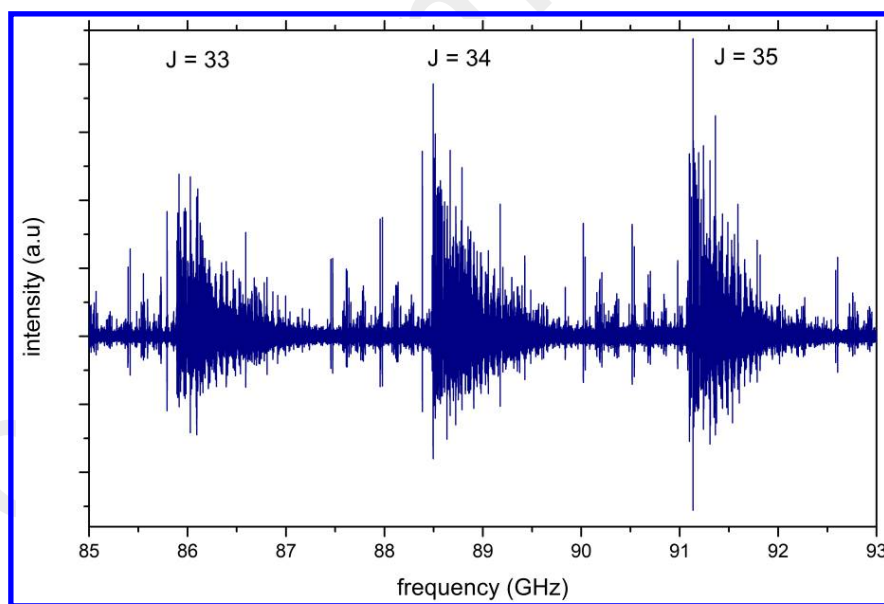


Figure 2: The rotational spectrum of HBN between 85 GHz and 93 GHz. The **band heads** of ${}^aR_{0,1}$ series transitions can be clearly distinguished. Since the band head frequency may be approximated as $(B + C)(J' + 1)$ one can easily provide the assignment of the quantum number J' for each series, as well as the initial correction for B and C rotational constants.

At first, the rotational lines of each tunneling substate were fitted separately using stan-

1
2
3 dard Watson S-reduction Hamiltonian. However, the $K_a = 2$ lines of 0^+ state were found
4 perturbed, as one could not fit these lines within experimental accuracy using a single state
5 approach. To treat the tunneling splittings, we applied the method based on reduced-axis-
6 system (RAS) method proposed by Pickett.³⁴ It is well suited for molecules with a double
7 minimum-potential. In matrix form, in the basis of individual wavefunctions of each tunnel-
8 ing substate $|0^+\rangle$ and $|0^-\rangle$, the RAS Hamiltonian has the following form:
9
10
11
12
13
14

$$15 \quad H = \begin{pmatrix} H_{\text{rot}} - H_{\Delta} & H_I \\ H_I & H_{\text{rot}} + H_{\Delta} \end{pmatrix} \quad (3)$$

16
17 In Eq.3, H_{rot} is the standard Watson S-reduction Hamiltonian in the I^r coordinate repre-
18 sentation, H_{Δ} is the part of the Hamiltonian that allows fitting averaged rotational constants
19 for both tunneling substates:
20
21
22
23
24
25
26
27
28

$$29 \quad H_{\Delta} = E^* + E_J^* P^2 + E_K^* P_z^2 + E_2^* (P_+^2 + P_-^2) + \dots \quad (4)$$

30
31 with the energy difference between two substates $\Delta E = 2E^*$. Such definition of the Hamil-
32 tonian has two main advantages. First, a unique set of rotational and centrifugal distortion
33 parameters permits an easier comparison with quantum chemical calculations. Second, this
34 method is more robust and avoids correlations between different rotational and Coriolis cou-
35 pling parameters. In Eq. 3, H_I is a perturbation Hamiltonian containing $F_{xy}(P_x P_y + P_y P_x)$,
36 and $F_{yz}(P_y P_z + P_z P_y)$ terms, and their centrifugal distortion corrections. These non-diagonal
37 terms determine the orientation of the reduced axis system with respect to the principal axis
38 system.
39
40
41
42
43
44
45
46
47

48 The convergence of non-linear least-squares fit strongly depends on initial conditions. In
49 the case of HBN, among the terms of the RAS Hamiltonian, those describing the interaction
50 between tunneling substates, ΔE and F , initially were rather poorly determined. This
51 may be a typical situation for the first stage of spectral analysis with limited number of
52 assigned lines. Due to relatively weak μ_c dipole moment component and dense spectrum,
53
54
55
56
57
58
59
60

1
2
3 the assignment of $0^+ \leftrightarrow 0^-$ transitions of HBN was not straightforward and therefore, the
4 only information on the ΔE term were the results of quantum chemical calculations. The
5 F terms, describing orientation of the RAS with respect to the principal inertia axes were
6 roughly estimated from optimized molecular geometry. In addition, ΔE and F terms are
7 highly correlated, and least-squares fit may diverge rather rapidly, when the initial values of
8 these two parameters are far from global solution.
9

10
11 To search for the global solution, we applied the following method. To remove the
12 correlation between ΔE and F in the least-squares fit, one of the parameters is fixed. The
13 method consists in performing a series of fits with different values of the fixed parameter
14 (FP). The range of FP values in the series of fits is chosen on the basis of reasonable initial
15 approximation, e.g. from quantum chemical calculations. Then, one can plot the root-mean-
16 square (rms) deviation of each fit as a function of FP. The global solution should correspond
17 to the minimum on the rms(FP) plot. It should be noted, that the method allows finding
18 initial convergence point for global solution provided that the Hamiltonian does not contain
19 redundant terms that may effectively take the Coriolis interaction into account. The method
20 was implemented in a computer program. The program prepares a set of input .par files with
21 different FP values for SPFIT code. Then, the program starts SPFIT for each .par file from
22 the set, and performs the analysis of corresponding generated .fit file with the results of the
23 least-squares fit. The program output contains the values of rms, FP, number of iterations,
24 as well as the information whether the convergence was achieved.
25
26
27
28
29
30
31
32
33
34
35
36
37
38
39
40
41
42

43 In the case of searching for global solution of the torsion-rotational problem of *gauche*-
44 HBN, we preferred to fix the ΔE parameter as it has direct physical meaning of the energy
45 difference between tunneling substates. We performed a series of fits with ΔE parameters
46 fixed to the values in the range between 100 and 230 GHz that encompasses the value
47 of 173.3 GHz determined from quantum chemical calculations. **The dataset of fitted**
48 **lines included 49 transitions with $18 \leq J \leq 26$, and $K_a \leq 2$. The Hamiltonian**
49 **model employed in the initial series of fits contained 13 varied parameters: three**
50
51
52
53
54
55
56
57
58
59
60

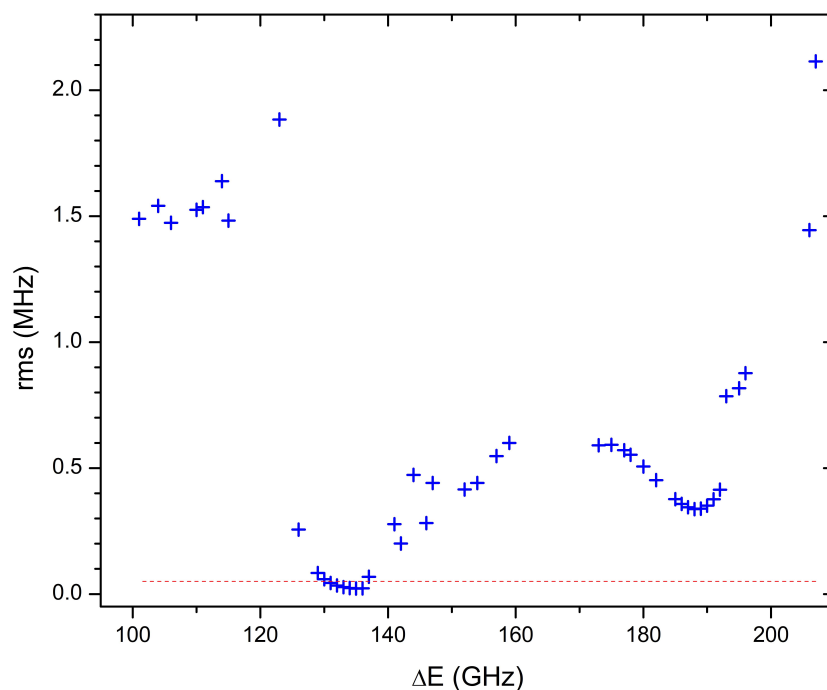


Figure 3: Root-mean-square deviation of least-squares fits of the experimental data to the model Hamiltonian of Eq. 3 as a function of the energy difference ΔE between two tunneling substates. The ΔE was fixed in each fit. The points represent the results of the fits in which convergence was achieved after a maximum of 15 iterations. **The dashed line corresponds to experimental accuracy.**

1
2
3 **rotational constants and D_J , d_1 , and d_2 centrifugal distortion parameters for each**
4 **tunneling substate, as well as F_{xy} coupling constant.** Individual rms of the fits plotted
5 as function of ΔE are presented on Fig. 3. The points on Fig. 3 correspond to the results
6 of the fits in which convergence was achieved after a maximum of 15 iterations. For all
7 others ΔE values in the range 100 - 230 GHz least-squares fits diverged. The rms(ΔE) plot
8 contains two distinct minima. The first minimum in the vicinity of 189 GHz corresponds to a
9 local solution that is rather far from experimental accuracy represented on Fig. 3 by dashed
10 line. The second solution around 135 GHz can be considered as a global one, as it provides
11 overall rms lower than experimental accuracy. The resultant values of ΔE and F parameters
12 determined from the fit with the lowest rms were considered as good initial approximation.
13 At this stage, one may now let ΔE parameter to vary in order to refine the global solution.
14 In the case of *gauche*-HBN, the ΔE value refined after obtaining initial approximation at
15 135 GHz permitted to locate in the spectrum the origins of ${}^cQ_{1,0}$ bands that connect two
16 tunneling substates. The assignment and fit of rotational transitions of such bands leded
17 to accurate determination of ΔE , and removed its correlation with F parameters.
18
19
20
21
22
23
24
25
26
27
28
29
30
31
32

33 The following assignment was performed in a usual "bootstrap" manner starting from
34 the results of the initial analysis and progressively adding newly assigned lines, and when
35 needed, also adding new parameters in the model. In total, we assigned almost 3000 dis-
36 tinct frequency lines of *gauche*-HBN. These lines were fitted with overall rms of 0.035 MHz
37 using the model of the RAS Hamiltonian that contains 34 parameters. The complete list of
38 measured rotational transitions of *gauche*-HBN in the ground vibrational state is available
39 in Supporting Information.
40
41
42
43
44
45
46

47 The values of J quantum numbers of transitions included in the fit range from 8 up to 129.
48 As for the values of K_a , the dataset of fitted lines contains the rotational transitions with
49 $K_a \leq 17$. The limitation in K_a was necessary as we were not able to fit within experimental
50 accuracy the lines with higher values of K_a . In attempt to fit these lines, one had to include
51 in the model 10th order rotational terms. The determined values of P^{10} terms had the
52
53
54
55
56
57
58
59
60

Table 2: Rotational parameters of gauche conformer of HBN

Parameters	Rotation		Torsion	
	Experiment	Theory	Parameters	Experiment
A (MHz)	26133.1112(37) ^a	25989.27	ΔE (MHz)	136489.634(33)
B (MHz)	1327.134505(64)	1325.56	E_J^* (MHz)	0.2041645(74)
C (MHz)	1275.291296(60)	1273.50	E_K^* (MHz)	-8.97442(52)
D_J (kHz)	0.1539735(73)	0.1539	E_2^* (MHz)	0.031360(12)
D_{JK} (kHz)	-19.6762(10)	-19.02	E_{JJ}^* (kHz)	-0.00043230(89)
D_K (kHz)	1893.157(45)	1785.	E_{JK}^* (kHz)	-0.05429(32)
d_1 (kHz)	-0.0235088(32)	-0.0231	E_{KK}^* (kHz)	2.8111(44)
d_2 (kHz)	-0.0014701(14)	-0.00133	E_{2J}^* (Hz)	-0.09999(69)
H_J (Hz)	0.00018783(55)		F_{yz} (MHz)	20.77149(38)
H_{JK} (Hz)	-0.018962(67)		F_{xy} (MHz)	-0.41929(28)
H_{KJ} (Hz)	-1.4549(67)		F_{yzJ} (kHz)	0.014185(87)
H_K (Hz)	273.68(18)		F_{yzK} (kHz)	-5.751(61)
h_1 (mHz)	0.04955(11)		F_{xyJ} (kHz)	-0.001791(15)
h_2 (mHz)	0.007578(82)		F_{xyK} (kHz)	-4.161(95)
h_3 (mHz)	0.001110(22)		F_{2xy} (kHz)	-0.001307(25)
L_J (μ Hz)	-0.000329(14)			
L_{JJK} (μ Hz)	0.0449(17)			
L_{JK} (mHz)	-0.01096(20)			
L_{KJ} (mHz)	-0.305(12)			

^a Numbers in parentheses are two standard deviations in the same units as the last digit.

1
2
3 same orders of magnitude as the values of corresponding P^8 terms which indicated that
4 the Hamiltonian did not converge properly. This problem may be explained by relatively
5 high energies of the levels with $K_a > 17$. According to our estimations, these levels lie well
6 above the barrier to OH torsion and correspond to almost free rotation of hydroxyl hydrogen.
7 Therefore, such high- K_a levels cannot be described by the same potential energy terms as
8 low- K_a levels. In this case, one has to redefine the PES, which also implies the redefinition of
9 centrifugal distortion parameters, and consequently may lead to the Hamiltonian convergence
10 problems.
11

12
13 This problem may also be considered from the point of view of the RAS approach.
14 The RAS method uses first order perturbation theory to treat the internal motion with
15 double minimum potential. As the amplitude of vibrational motion may be linked to the
16 barrier height, one may conclude that the RAS method is suitable for molecules with high
17 barrier to internal rotation. Previously it was also shown that the RAS method is closely
18 related to internal-axis-method (IAM) type models developed by Hougen and coworkers³⁵⁻³⁷
19 for molecules with several large amplitude motions. Indeed, both approaches consider the
20 problem in terms of a phenomenological Hamiltonian, and a set of splittings which arise
21 from tunneling of the system between equivalent non-superimposable configurations of the
22 molecule. Both methods allow taking into account the Coriolis interaction between the
23 tunneling motion and the overall rotation of the molecule. As the RAS method, the IAM
24 formalism provides good convergence in high-barrier cases, because it requires the localization
25 of individual vibrational wave functions in each minimum on PES. HBN may be considered as
26 a molecule with medium or low barrier to internal rotation, as the first excited OH-torsional
27 state lies very close to the top of the barrier. Therefore, the application of RAS or IAM-type
28 models has some limitations, as it was found in the present study.
29

30
31 The results of the fit are presented in Table 2. The calculated energy difference $\Delta E =$
32 136489.634(33) MHz is lower than predicted from quantum chemical calculations suggest-
33 ing that the barrier to OH torsion should be slightly higher than the value obtained from
34
35
36
37
38
39
40
41
42
43
44
45
46
47
48
49
50

1
2
3 vibrationaly corrected 1D-PES. The results of the present study may be compared to the
4 results of similar molecule 2-hydroxyacetonitrile (HOCH_2CN , HAN)³⁸. For HAN, the same
5 variational approach in solving the vibrational Hamiltonian yielded theoretical value of ΔE
6 which was lower than experimentally determined ΔE . Recently, we studied the problem
7 of OH torsion for conformer III of methoxymethanol³⁹. Theoretical calculations suggested
8 that the barrier to OH torsion for conformer III is 492 cm^{-1} , being higher than for HAN.
9 Therefore, one had to search for the initial solution with ΔE lower than the corresponding
10 value for HAN. Using this assumption we rapidly found the initial convergence point with
11 ΔE around 90 GHz, and further refinement yielded the value of $\Delta E = 90678.0(11)\text{ MHz}$
12 for conformer III of methoxymethanol. In all these cases, theoretical calculations provided a
13 good starting point in searching for initial global solution of the torsional-rotational problem
14 using the method described above.
15
16
17
18
19
20
21
22
23
24
25
26
27
28

29 Conclusions

30
31
32 The results of this study represent the first spectroscopic characterization of *gauche* con-
33 formation of 4-hydroxy-2-butyne nitrile in the frequency range up to 500 GHz. We assigned
34 and analyzed the rotational spectrum of the most stable *gauche* conformation of HBN. The
35 assignment was complicated by tunneling splittings owing to large amplitude motion of the
36 OH group. The analysis was aided by high-level quantum chemical calculations, and by
37 the method of finding the global solution of least-squares fit. The latter proved to be very
38 useful tool for the initial stage of spectral analysis, in the case when the information on the
39 torsion-rotational part of the problem is limited by the results of theoretical calculations.
40 The final set of molecular parameters allow accurate frequency predictions throughout all
41 the frequency range where strong lines of HBN may be found, including interpolation of
42 spectral predictions below 50 GHz. The calculated frequency predictions at temperature
43 of 300 K are available in Supporting Information. Thus, the results of the present study
44
45
46
47
48
49
50
51
52
53
54
55
56
57
58
59
60

1
2
3 represent a solid basis for the searches of HBN in the interstellar medium.
4
5
6

7 8 **Acknowledgement** 9

10 This work was supported by the French Programme National "Physique et Chimie du Milieu
11 Interstellaire" (PCMI) of CNRS/INSU with INC/INP co-funded by CEA and CNES, and
12 by the ANR-13-BS05-0008 IMOLABS of the French Agence Nationale de la Recherche. The
13 authors also thank the projects FIS2013-40626-P and FIS2016-76418-P (Spanish ministry of
14 economy) and CESGA and CTI-CSIC computers centers.
15
16
17
18
19
20
21
22

23 **Supporting Information Available** 24 25

26 Measured frequencies, and calculated predictions of the rotational spectrum of *gauche*-HBN
27 up to 500 GHz. This material is available free of charge via the Internet at [http://pubs.
28 acs.org/](http://pubs.acs.org/).
29
30
31
32
33

34 **References** 35 36

- 37 (1) Turner, B. Detection of interstellar cyanoacetylene. *The Astrophysical Journal* **1971**,
38 *163*, L35.
39
40
41
42 (2) Morris, M.; Turner, B.; Palmer, P.; Zuckerman, B. Cyanoacetylene in dense interstellar
43 clouds. *The Astrophysical Journal* **1976**, *205*, 82–93.
44
45
46
47 (3) Clark, F.; Brown, R.; Godfrey, P.; Storey, J.; Johnson, D. Detection of interstellar
48 vibrationally excited cyanoacetylene. *The Astrophysical Journal* **1976**, *210*, L139–L140.
49
50
51
52 (4) Walmsley, C. M.; Winnewisser, G.; Toelle, F. Cyanoacetylene and cyanodiacetylene in
53 interstellar clouds. *Astronomy and Astrophysics* **1980**, *81*, 245–250.
54
55
56
57
58
59
60

- 1
2
3 (5) Mauersberger, R.; Henkel, C.; Sage, L. Dense gas in nearby galaxies. III-HC3N as an
4 extragalactic density probe. *Astronomy and Astrophysics* **1990**, *236*, 63–68.
5
6
7
8 (6) Lis, D.; Mehringer, D.; Benford, D.; Gardner, M.; Phillips, T.; Bockelée-Morvan, D.;
9 Biver, N.; Colom, P.; Crovisier, J.; Despois, D. et al. New Molecular Species in Comet
10 C/1995 O1 (Hale-Bopp) Observed with the Caltech Ssubmillimeter Observatory. *Earth,*
11 *Moon, and Planets* **1997**, *78*, 13–20.
12
13
14
15
16 (7) Kunde, V.; Aikin, A.; Hanel, R.; Jennings, D.; Maguire, W.; Samuelson, R. C4H2,
17 HC3N and C2N2 in Titan’s atmosphere. *Nature* **1981**, *292*, 686–688.
18
19
20
21 (8) Cordiner, M.; Nixon, C.; Teanby, N.; Irwin, P.; Serigano, J.; Charnley, S.; Milam, S.;
22 Mumma, M.; Lis, D.; Villanueva, G. et al. ALMA Measurements of the HNC and
23 HC3N Distributions in Titan’s Atmosphere. *The Astrophysical Journal Letters* **2014**,
24 *795*, L30.
25
26
27
28
29 (9) Cherchneff, I.; Glassgold, A. E. The formation of carbon chain molecules in IRC+
30 10216. *The Astrophysical Journal* **1993**, *419*, L41.
31
32
33
34 (10) Cherchneff, I.; Glassgold, A. E.; Mamon, G. A. The formation of cyanopolyne
35 molecules in IRC+ 10216. *The Astrophysical Journal* **1993**, *410*, 188–201.
36
37
38
39 (11) Trolez, Y.; Guillemin, J.-C. Synthesis and characterization of 2, 4-pentadienenitrile - A
40 key compound in space science. *Angewandte Chemie International Edition* **2005**, *44*,
41 7224–7226.
42
43
44
45 (12) Coupeaud, A.; Kołos, R.; Couturier-Tamburelli, I.; Aycard, J.; Piétri, N. Photochemical
46 synthesis of the cyanodiacetylene HC5N: A cryogenic matrix experiment. *The Journal*
47 *of Physical Chemistry A* **2006**, *110*, 2371–2377.
48
49
50
51
52 (13) Kerisit, N.; Toupet, L.; Trolez, Y.; Guillemin, J.-C. Methylcyanobutadiyne: Synthesis,
53
54
55
56
57
58
59
60

- X-ray Structure and Photochemistry; Towards an Explanation of Its Formation in the Interstellar Medium. *Chemistry-A European Journal* **2013**, *19*, 17683–17686.
- (14) Kerisit, N.; Rouxel, C.; Colombel-Rouen, S.; Toupet, L.; Guillemin, J.-C.; Trolez, Y. Synthesis, Chemistry, and Photochemistry of Methylcyanobutadiyne in the Context of Space Science. *The Journal of Organic Chemistry* **2016**, *81*, 3560–3567.
- (15) Askeland, E.; Møllendal, H.; Uggerud, E.; Guillemin, J.-C.; Aviles Moreno, J.-R.; Demaison, J.; Huet, T. R. Microwave spectrum, structure, and quantum chemical studies of a compound of potential astrochemical and astrobiological interest: Z-3-amino-2-propenenitrile. *The Journal of Physical Chemistry A* **2006**, *110*, 12572–12584.
- (16) Møllendal, H.; Margulès, L.; Belloche, A.; Motiyenko, R.; Konovalov, A.; Menten, K.; Guillemin, J.-C. Rotational spectrum of a chiral amino acid precursor, 2-aminopropionitrile, and searches for it in Sagittarius B2 (N). *Astronomy & Astrophysics* **2012**, *538*, A51.
- (17) Møllendal, H.; Margulès, L.; Motiyenko, R. A.; Larsen, N. W.; Guillemin, J.-C. Rotational spectrum and conformational composition of cyanoacetaldehyde, a compound of potential prebiotic and astrochemical interest. *The Journal of Physical Chemistry A* **2012**, *116*, 4047–4056.
- (18) Friberg, P.; Hjalmarsen, A.; Guelin, M.; Irvine, W. Interstellar C₃N-Detection in Taurus dark clouds. *The Astrophysical Journal* **1980**, *241*, L99–L103.
- (19) Ohishi, M.; Irvine, W. M.; Kaifu, N. Molecular abundance variations among and within cold, dark molecular clouds (rp). *Astrochemistry of Cosmic Phenomena*. 1992; p 171.
- (20) Fleming, F. F.; Gudipati, V.; Steward, O. W. Alkynenitriles: stereoselective chelation controlled conjugate addition–alkylations. *Tetrahedron* **2003**, *59*, 5585–5593.

- 1
2
3
4
5
6
7
8
9
10
11
12
13
14
15
16
17
18
19
20
21
22
23
24
25
26
27
28
29
30
31
32
33
34
35
36
37
38
39
40
41
42
43
44
45
46
47
48
49
50
51
52
53
54
55
56
57
58
59
60
- (21) Zakharenko, O.; Motiyenko, R. A.; Margulès, L.; Huet, T. R. Terahertz spectroscopy of deuterated formaldehyde using a frequency multiplication chain. *Journal of Molecular Spectroscopy* **2015**, *317*, 41–46.
- (22) Werner, H.; Knowles, P.; Knizia, G.; Manby, F.; Schütz, M.; Celani, P.; Korona, T.; Lindh, R.; Mitrushenkov, A.; Rauhut, G. et al. MOLPRO, version 2012.1, a package of ab initio programs, 2012; see <http://www.molpro.net>. *MOLPRO, version 2012.1, a package of ab initio programs, 2012; see http://www.molpro.net* **2012**,
- (23) Frisch, M. J.; Trucks, G. W.; Schlegel, H. B.; Scuseria, G. E.; Robb, M. A.; Cheeseman, J. R.; Scalmani, G.; Barone, V.; Mennucci, B.; Petersson, G. A. et al. Gaussian 09, revision D.01. 2009.
- (24) Knizia, G.; Adler, T. B.; Werner, H.-J. Simplified CCSD (T)-F12 methods: Theory and benchmarks. *J. Chem. Phys.* **2009**, *130*, 054104.
- (25) Werner, H.-J.; Adler, T. B.; Manby, F. R. General orbital invariant MP2-F12 theory. *J. Chem. Phys.* **2007**, *126*, 164102.
- (26) Kendall, R. A.; Dunning Jr, T. H.; Harrison, R. J. Electron affinities of the first-row atoms revisited. Systematic basis sets and wave functions. *The Journal of Chemical Physics* **1992**, *96*, 6796–6806.
- (27) Senent, M. Ab initio study of the torsional spectrum of glycolaldehyde. *The Journal of Physical Chemistry A* **2004**, *108*, 6286–6293.
- (28) Barone, V. Anharmonic vibrational properties by a fully automated second-order perturbative approach. *The Journal of Chemical Physics* **2005**, *122*, 014108.
- (29) Császár, A. G.; Szalay, V.; Senent, M. L. Ab initio torsional potential and transition frequencies of acetaldehyde. *The Journal of Chemical Physics* **2004**, *120*, 1203–1207.

- 1
2
3
4 (30) Senent, M.; Dalbouha, S.; Cuisset, A.; Sadovskii, D. Theoretical Spectroscopic Char-
5 acterization at Low Temperatures of Dimethyl Sulfoxide: The Role of Anharmonicity.
6 *The Journal of Physical Chemistry A* **2015**, *119*, 9644–9652.
7
8
9
10 (31) Raghavachari, K.; Trucks, G. W.; Pople, J. A.; Head-Gordon, M. A fifth-order per-
11 turbation comparison of electron correlation theories. *Chemical Physics Letters* **1989**,
12 *157*, 479–483.
13
14
15
16 (32) Senent, M. Ab Initio Determination of the Roto-Torsional Energy Levels of trans-1, 3-
17 Butadiene. *Journal of Molecular Spectroscopy* **1998**, *191*, 265–275.
18
19
20
21 (33) Senent, M. Determination of the kinetic energy parameters of non-rigid molecules.
22 *Chemical Physics Letters* **1998**, *296*, 299–306.
23
24
25
26 (34) Pickett, H. M. Vibration-Rotation Interactions and the Choice of Rotating Axes for
27 Polyatomic Molecules. *The Journal of Chemical Physics* **1972**, *56*, 1715–1723.
28
29
30
31 (35) Hougen, J. T. A generalized internal axis method for high barrier tunneling problems,
32 as applied to the water dimer. *Journal of Molecular Spectroscopy* **1985**, *114*, 395–426.
33
34
35
36 (36) Ohashi, N.; Hougen, J. T. The torsional-wagging tunneling problem and the torsional-
37 wagging-rotational problem in methylamine. *Journal of Molecular Spectroscopy* **1987**,
38 *121*, 474–501.
39
40
41
42 (37) Coudert, L.; Hougen, J. Tunneling splittings in the water dimer: Further development
43 of the theory. *Journal of Molecular Spectroscopy* **1988**, *130*, 86–119.
44
45
46
47 (38) Margulès, L.; McGuire, B. A.; Senent, M. L.; Motiyenko, R. A.; Remijan, A.;
48 Guillemin, J. C. Submillimeter spectra of 2-hydroxyacetonitrile (glycolonitrile;
49 HOCH₂CN) and its searches in GBT PRIMOS observations of Sgr B2 (N). *Astron-*
50 *omy & Astrophysics* **2017**, *601*, A50.
51
52
53
54
55
56
57
58
59
60

- 1
2
3 (39) Motiyenko, R. A.; Margulès, L.; Despois, D.; Guillemin, J.-C. Laboratory spectroscopy
4 of methoxymethanol in the millimeter-wave range. *Phys. Chem. Chem. Phys.* **2018**, *20*,
5 5509–5516.
6
7
8
9
10
11
12
13
14
15
16
17
18
19
20
21
22
23
24
25
26
27
28
29
30
31
32
33
34
35
36
37
38
39
40
41
42
43
44
45
46
47
48
49
50
51
52
53
54
55
56
57
58
59
60

Graphical TOC Entry

